



HAL
open science

Point Clouds Segmentation of Mixed Scenes with Archeological Standing Remains: A Multi-Criteria and Multi-Scale Iterative Approach

Rachel Opitz, Laure Nuninger

► **To cite this version:**

Rachel Opitz, Laure Nuninger. Point Clouds Segmentation of Mixed Scenes with Archeological Standing Remains: A Multi-Criteria and Multi-Scale Iterative Approach. *International Journal of Heritage in the Digital Era*, 2014, 3 (2), pp.287-304. 10.1260/2047-4970.3.2.287 . halshs-01099810

HAL Id: halshs-01099810

<https://shs.hal.science/halshs-01099810>

Submitted on 7 Jun 2023

HAL is a multi-disciplinary open access archive for the deposit and dissemination of scientific research documents, whether they are published or not. The documents may come from teaching and research institutions in France or abroad, or from public or private research centers.

L'archive ouverte pluridisciplinaire **HAL**, est destinée au dépôt et à la diffusion de documents scientifiques de niveau recherche, publiés ou non, émanant des établissements d'enseignement et de recherche français ou étrangers, des laboratoires publics ou privés.



Distributed under a Creative Commons Attribution - NonCommercial - NoDerivatives 4.0 International License

Point clouds segmentation of mixed scenes with archeological standing remains: a multi-criteria and multi-scale iterative approach

R. Opitz ^a and L. Nuninger ^b

^a CAST, University of Arkansas, Fayetteville, AR USA / LEA ModelTER / MSHE
Ledoux USR 3124, UFC, Besançon, France – ropitz@cast.uark.edu

^b Chrono-Environnement UMR 6249 / LEA ModelTER / MSHE Ledoux USR 3124,
CNRS, Besançon, France – laure.nuninger@univ-fcomte.fr

ABSTRACT

The integration of Airborne Laser Scanning survey into archaeological research and cultural heritage management has substantially added to our knowledge of archaeological remains in forested areas, and is changing our understanding of how these landscapes functioned in the past. Further, the results of ALS-based surveys of woodlands can now potentially be incorporated into micro-regional and landscape scale studies which rely on survey data, making an important contribution to our understanding of settlement patterns and land use – but doing so requires us to recognize and manage a host of biases inherent in ALS-based survey data. While many types of archaeological remains manifest as micro-topography, several important classes of features commonly appear as standing remains. The identification of these remains is important for archaeological prospection surveys based on ALS data. Standing structures in mixed scenes with vegetation are not well addressed by standard classification approaches. In this paper we propose an approach to the identification of these structures in the point cloud based on multi-scale measures of roughness, and measures of local density and normal orientation. We demonstrate this approach using discrete-return ALS data collected in the Franche-Comte region of France.

1. INTRODUCTION

1.1 Why identify standing archaeological remains in woodland and scrub landscapes?

The integration of Airborne Laser Scanning (ALS) survey into archaeological research and cultural heritage management has substantially added to our knowledge of archaeological remains in forested areas, and is changing our understanding of how these landscapes functioned in the past. Further, the results of ALS-based surveys of woodlands can now potentially be incorporated into micro-regional and landscape scale studies which rely on survey data, making an important contribution to our understanding of settlement patterns and land use over time – but doing so requires us to recognize and manage a host of biases inherent in ALS-based survey data. Ameliorating these biases requires methodological development, especially in point clouds segmentation, because points identified as terrain are the basic data for the digital terrain model, and for models of surface objects, used for archaeological analysis and interpretation.

To date, the majority of the remains identified through ALS can be characterized as earthworks-slight or sometimes substantial local variations in micro-topography [1]. While many types of archaeological remains manifest as micro-topography, several important classes of features commonly appear as standing remains. These remains typically represent structures from the Roman, Medieval and early Modern periods in Old World (European) archaeology, and a failure to regularly identify them in ALS could result in the underrepresentation of these periods. This problem is not restricted to Continental and Mediterranean Europe; standing remains constitute important evidence for settlement and other activities across a spectrum of culturalhistorical periods globally, for example Puebloan archaeology of the Southwest United States[2], Mayan archaeology in Central America [3], or Angkor Period archaeology in Cambodia [4]. Broadly we may say that stone built architectural remains are essential to the characterization of the site distribution and landscape organization of many proto-historic and historic periods.

Problematically for archaeologists, standing archaeological remains are frequently found in areas characterized by dense low vegetation. In fact, the presence of standing remains can encourage the growth of low and medium height vegetation. The presence of dense scrub surrounding standing remains results in poor visibility on the ground, and can even prevent access to the remains in extreme, but numerous, cases. This introduces a significant bias into pedestrian surveys.

Equally, standing structures in mixed scenes with vegetation are not well addressed by standard classification approaches developed to identify bare earth (terrain), individual trees or plot characteristics, or buildings (roofed structures). These structures are typically mixed into the low- or medium- vegetation classes by terrain-seeking algorithms, and into ‘understory’ by vegetation building-extraction algorithms. Thus, in ALS-based surveys we have a parallel bias to that seen in pedestrian surveys: poor visibility of standing remains and a low likelihood that they will be noticed and recorded.

In this paper we present a method for the identification of standing archaeological remains in mid-resolution discrete return ALS data. We note that while in ALS-based survey, full-waveform lidar data can provide a relatively straightforward path to distinguishing standing structures from the surrounding vegetation based on echo-width filtering [5], the substantial archive of discrete return ALS data must be treated using purely geometric measures, as in the method proposed below. Further, echo-width filtering is not always sufficient to distinguish small archaeological remains from surrounding vegetation, and the best approach for full waveform lidar classification may be one that combines echo width filtering and the approach proposed in this paper. The case studies presented here use ALS data collected for temperate European landscapes, but the results should be applicable in Mediterranean landscapes where the detection of these remains has been particularly difficult [6][7] and elsewhere.

2. METHODS AND ALGORITHMS

2.1 Summary of the proposed method

In this paper we propose a method to segment ALS point clouds representing mixed scenes containing returns from terrain, vegetation, and standing archaeological remains using purely geometric measures. This method has been developed using ALS data at a nominal density of 8 pts/m², a resolution likely to become increasingly available to researchers and managers through regional and national mapping schemes. In the proposed approach a point cloud representing a mixed scene containing terrain, vegetation and standing archaeological remains is selected for analysis. The point cloud was initially classified using a terrain-seeking algorithm implemented in TerraScan (TerraSolid software). TerraScan relies on an adaptation of Axelsson’s algorithm, which discriminates between terrain and vegetation points using a series of adaptive TINs [8]. This algorithm is well suited for large scale terrain/non-terrain segmentation of point clouds, but significantly less well suited to identifying individual components within the vegetation segment of the point cloud. The pre-classified point cloud is then segmented on the basis of three criteria: roughness (a measure of dimensionality), local density, and normal orientation. For the examples presented here all roughness calculations were performed in CloudCompare, and density and normal calculations were performed in Meshlab. Regions of points representing standing remains, which were initially identified as vegetation by the Terrascan algorithm, are reclassified on the basis of their low roughness, as calculated at multiple scales, low density as compared to terrain points, and consistent normal orientation as compared to vegetation points.

In addition to presenting our core, original approach using multi-scale roughness, as presented at CIPA 2013 [9] in this paper we demonstrate that the results obtained using Brodu and Lague et al.’s metric, as implemented in CANUPO [16], can be used as an alternative to roughness, and serve as an alternative input to the segmentation steps based on density and normal orientation. This is consistent with the point made below, that the ideal measure of dimensionality (how 1D, 2D, or 3D a geometry is) is not established. Presenting the use of an alternative metric to characterize dimensionality serves to emphasize that our approach is not strongly dependent on the specifics of the dimensionality metric used, or reliant on how it is calculated in a specific software program - the principle of segmentation based on dimensionality characterized at multiple scales combined with an opening operation is robust. Further, we demonstrate that in the special case of mixed scenes with architecture and vegetation, further segmentation on density and normal orientation is necessary, as implemented in our approach.

2.2 Related Approaches to Mixed Scenes

2.2.1 General ALS vs TLS classification approaches

The segmentation of point clouds created through laserscanning is a well-established problem. A number of methods have been developed for ALS point clouds (see [10] [11] for an overview, [7] for an overview as applied to archaeology) and for TLS point clouds (see [12] [13]). While we are applying the approach proposed here to ALS data, the inspiration for the proposed method is drawn primarily from approaches to the segmentation of TLS data. ALS classification strategies for separating terrain, vegetation and buildings in rural scenes, operate on the principle of identifying a more or less continuous surface, the ground, and then identifying other objects in relation to that primary surface. This is not particularly useful in our application, as vegetation and standing remains classes will be mixed, as noted above. Urban scene segmentation is now treated separately in the ALS literature (see [14] [15] for urban scene segmentation), and our proposed approach is related to some urban scene segmentation strategies, notably those using contextual classification strategies. TLS segmentation has generally followed a connected components approach, segmenting a point cloud into amorphous patches based on local statistical similarities, rather than searching for surfaces. The identification of specific forms in the point cloud is carried out on a case-by-case basis, with a signature developed for each form, e.g. cylindrical forms to detect branches and trunks in vegetation scenes. Our method can be understood in this context, and addresses the class of forms which typically describe standing remains, as they appear in mixed scenes with low and mid height vegetation.

2.2.2 Multi-scale Segmentation applied to TLS point clouds of natural scenes

TLS scans of natural scenes that contain multiple elements, including vegetation, stones, and soil, pose many of the same problems as mixed natural scenes in ALS, including heterogeneity in the morphological characteristics of each class of features, random orientation of structural elements, and local shadow effects in the point cloud. Consequently the fundamentals of the approaches developed to segment scenes are similar. The approach developed by Lague et al. [16] [17], like the one presented here, uses a measure of multi-scale dimensionality to characterize the local geometry of the neighbourhood around each point. They develop a metric for multi-scale dimensionality based on the dimensionality of a local neighbourhood sphere at varying scales around each point. The metric implemented by Brodu and Lague is conceptually close to the roughness metric used in our approach, in that it describes the local dimensionality of part of a point cloud.

2.2.3 Hierarchical Segmentation of ALS of Urban Scenes:

The classification of urban scenes in ALS data relies of different algorithms from those used for rural scenes, and much work in this area focuses on correctly separating buildings, individual trees, and other structures from the terrain. Successful approaches to urban scene segmentation include wavelets (e.g. [18]), region growing (e.g. [19]) and RANSAC (e.g. [20]). Because the main features of interest, e.g. roofs and building walls, are approximately planar, comparatively large, and not immediately surrounded by other off-terrain returns, and the vegetation present is usually individual or small groups of trees, without the presence of an understory, the approaches applied to urban scene segmentation are unlikely to be successful for separating standing archaeological remains from surrounding vegetation. Consequently, we do not review the methods in detail here.

2.1.1 A note on the metrics used

Roughness, a measure of spatial dimensionality, is calculated as the distance from each point to the locally (least square) fitted plane. This least square plane is computed with all the neighbouring points inside the sphere defined by a kernel radius. There are a number of alternative ways to calculate roughness. Various methods have been proposed including analysis of fractal dimensions [21], analyzing multi-scalar surface variograms [22][23], taking the standard deviation or range of elevations at a set scale, taking the multi-scalar variation of slope or curvature, or calculating variability after trend removal [24]. At the landscape scale Brubaker et al. [25] use four methods: standard deviation of slope, standard deviation of curvature, standard deviation of residual topography, and a pit fill metric, and note that different metrics will be appropriate at different scales and data resolutions. In the approach presented here in first instance we defined the kernel sizes based on the ALS data resolution, the scale of the remains studied, and by approximation guided by a series of tests.

Density is calculated as the radius of the sphere that contains a point and its x number of neighbours. Here we use 27 neighbours, representing a $3 \times 3 \times 3$ matrix around each point. Density can also be calculated as the number of points in a sphere or cube of a fixed radius. Because using a fixed radius requires testing to determine the appropriate radius to correctly represent local densities

in the point cloud, and choosing an inappropriate value can lead to misleading results, we prefer the neighbours-based approach.

Normal orientation is calculated at each point by selecting the closest neighbours and fitting a least squares plane on those points. The normal direction is perpendicular to the center of that plane, and stored as an unoriented normal on the vertex. In our approach we use 27 neighbours, typically allowing points within 1-1.5m to affect the orientation of the LS plane. There are several alternative means of calculating normal orientations for point clouds. Numerical optimizations, Area Weighted and Angle Weighted Averaging, and Voronoi diagrams [26] are well known solutions for the problem. Klasing et al. [27] present a good overview of the topic. While we have taken a simplistic approach to normal estimation, in more complex scenes with standing remains in close proximity at multiple orientations a more sophisticated approach may be needed.

The ideal measure of dimensionality to characterize 3D point clouds is a matter of debate. Fractal dimensionality and multifractal measures [28] and spatial correlation measures [29] have been used successfully on TLS data. Measures of roughness [30], density [31] and normal vector [32] are all regularly used to segment point clouds. In our approach the combination of roughness, density and normal orientation is preferred for distinguishing between approximately planar features (walls) and surrounding amorphous points (understory canopy) at relatively coarse resolutions compares to typical TLS data. The originality of our approach is in combining the measures, and iteratively calculating them across multiple scales in what is essentially an opening operation. The application to standing archaeological remains in mixed scenes is also, according to the literature, original.

2.1.2 Advantages of the proposed method

The proposed method has several advantages. First, computation is relatively rapid, because the 3D point cloud is treated directly and interpolation is avoided. Further, it is implementable using basic point cloud morphology metrics, meaning it can be carried out using a variety of open source software packages. Finally, only a few parameters need to be tested and set. Consequently, this approach can be implemented and adapted by researchers with limited computing resources, making it widely accessible. Further, the approach proposed here is flexible, in that the number of scales over which the calculation is performed can be varied, and the dimensionality metric, as discussed below, can be varied. This flexibility provides the means to adapt the filtering process to variations in conditions and to more or less complex study areas.

2.3 Detailed Description of the proposed method

2.3.1 Multi-scale iterative roughness calculations

In the first stage of the analysis local roughness values are calculated for each point at a scale s_1 . The roughness calculation is basic: at each point the roughness is calculated as equal to the distance between the point and the least square best fitting plane computed on its nearest neighbours. Points with fewer than 3 nearest neighbours within the sphere defined by the scale of the analysis are assigned an invalid scalar value (NaN) [33]. The Weibull distribution of the roughness values is calculated and points falling within one and two standard deviations (σ) of the distribution are identified. Points with roughness values exceeding 1σ of the roughness distribution are removed. Roughness values are then recalculated on the modified point cloud on a smaller spatial scale S_2 and points exceeding 1σ are again removed. In the third pass, the roughness values are recalculated on a larger scale S_3 . For ALS data at nominally 8 pts/m² and archaeological features at the 1-5m scale, S_1 is set at 5m. The parameters S_1 , S_2 and S_3 (figure 1) should be varied with respect to the scale of the standing remains sought and the nominal point

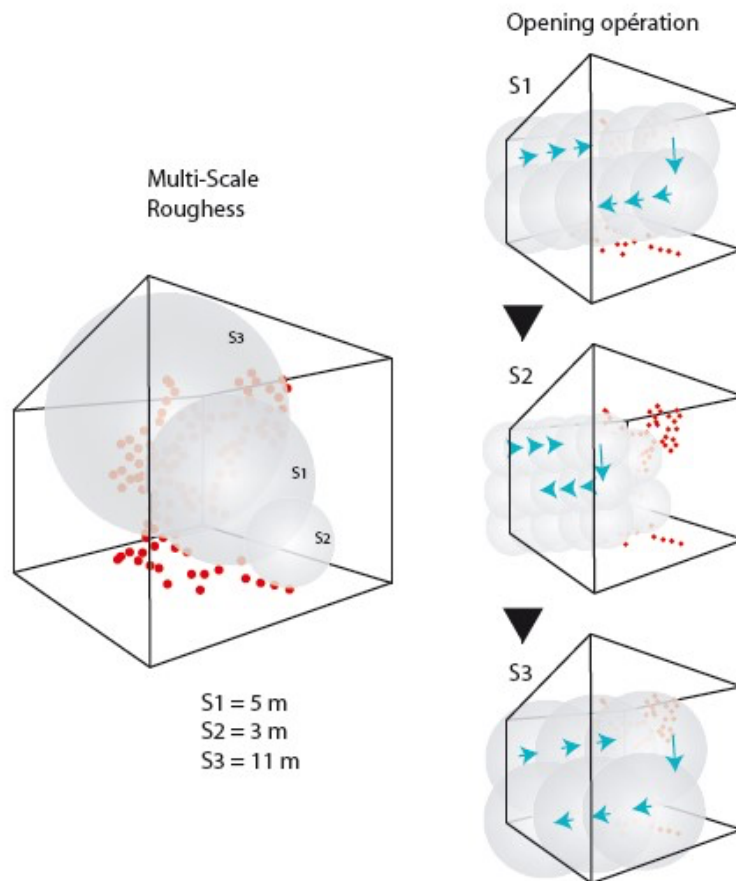


Figure 1: Spatial scales of analysis are represented as spheres, shown in relation to points from the point cloud.

density of the ALS data. (See below for a more general discussion on setting spatial scales of analysis.) For the case studies here, these parameters were set at 5, 3 and 11m. The selection of appropriate scale parameters is essential for the identification of standing architecture, and successful segmentation.

2.3.2 Alternative multi-scale spatial organization calculation using CANUPO

The results of the CANUPO program developed by Lague and Brodu work well as an alternative dimensionality input (alternative to roughness) in our approach. In their metric for each point a spherical neighborhood is computed at each scale of interest S , and a Principal Component Analysis (PCA) is performed on the re-centered point coordinates. The proportions of the eigenvalues of the PCA are used to define a measure of local dimensionality per scale. The full feature space, taken over multiple scales S is used in defining a classifier by projecting the data into a plane of maximal separability and then separating the classes in that plane [16].

2.3.3 Setting scales for multi-scale spatial organization calculations

Selecting appropriate scales for the multi-scale analysis, and the best number of neighbours for density and normal estimation calculations, is essential. To best select the scales appropriate to the data at hand, we begin by posing the question: at what scales do the different classes of objects look different? This is the key question, whether the roughness metric or a PCA of eigenvalues like that used in CANUPO or another metric of dimensionality is used. With data at a point spacing of 0.5m, at the 1m scale all objects will look morphologically similar because there are not many points available in a 1m radius and the number of possible shapes formed by these points is limited. At 5m meaningful differences between different classes of objects can be. At large scales, all shapes again begin to look similar. If the largest object in a scene is 15m tall and 8m wide, measurements of dimensionality at the 50m scale will not be meaningful. The aim is to select a range of scales from where spatial structures begin to emerge through where the largest object is smaller than the scale of analysis.

2.3.4 Segmentation on local density:

After initial segmentation of the point cloud based on multi-scale roughness, some points classified as vegetation remain in the scene. In the case studies here, these are clearly distinguishable by local point density. Local point densities are calculated on a 3x3x3 matrix of neighbours, and areas with low point densities, typically beyond 2σ in the distribution, are excluded. In the first two examples shown here, the use of a 3x3x3 matrix of neighbours produces good results. At other scales, it may be appropriate to vary the size of the neighbourhood. Optionally, a second pass of density segmentation may be undertaken, varying the size of the neighbour matrix.

2.3.5 Segmentation on normal orientation

After segmentation on local density remaining components can be separated into individual walls, and walls distinguished from terrain and any remaining vegetation components on the basis of normal orientation. Normal orientations are calculated for the resulting point cloud on the basis of each point's neighbours (26 neighbours are used in these calculations, representing an extended plane without a preferred orientation) [34]. The normal orientations are also used to differentiate between multiple structures at different orientations in the scene, on the basis of dominant normal orientation. As with local point densities, a second pass may be needed if features at substantially different scales are present in the scene.

2.4 Intended Applications

Archaeological sites on which standing remains may be expected are often identified in ALS data on the basis of more easily detected and visualized microtopographic features, e.g. mounds, ditches, cuttings, or platforms. This approach is intended for the analysis of forested scenes, where the potential for standing structures has been established. Consequently, the sites assessed for this paper are relatively small (under 1 ha.). This approach could be scaled up to address larger areas, but the problems of doing so, notably increased computational expense, are not addressed here.

3. CASE STUDY SITES

The approach developed to identify standing remains was tested at three sites with known standing structures. Two of these sites, Montfaucon and Bregille, contain substantial preserved walls, and the dominant scale of the standing archaeological features is 2-5m. At the third site, Chapelle des Buis, the dominant scale of standing features is 0.25-1m. All three sites were characterized by mixed deciduous forest with medium to dense understory canopies.



Figure 2: Standing remains at Montfaucon. Correct classification in the ALS point cloud (inset).

3.1 Montfaucon

3.1.1 Results using the original roughness metric

In the sample scene of the château and the deserted village of Montfaucon a single long wall, preserved to more than 2m in height and less than 1m in width is present (figure 2). 3.1.1. Results using the original roughness metric. After the roughness segmentation, as explained in the protocol above, some vegetation points remain (figure 3). Local point densities are calculated for the resulting point cloud and final remaining vegetation components, characterized by low point densities, are removed. Areas with consistent normal orientations (figure 3) define regions of terrain and standing architectural remains.

These regions of coherent normal orientations can be identified using a connected components calculation, a clustering approach, or by using a metric for similarity to neighbours. Terrain regions are confirmed by checking against the initial Terrascan classification of the point cloud. The resulting point cloud contains three classes: terrain, standing remains, and vegetation (figure 5).

3.1.2 Results using the alternative CANUPO metric

As with the original roughness metric, using CANUPO (scales S 1m-10m, 0.5m intervals) for the dimensionality metric points belonging to the wall class are correctly classified, and some vegetation points remain. These components, representing the strongly structured parts of the vegetation canopy, e.g. branches, have a similar roughness and density to those from wall components, and therefore remain after the density step. However, these components have normal oriented strongly toward the Z+ axis or less coherently oriented than those from the wall component, and are therefore removed through the normal orientation segmentation step (figure 4).

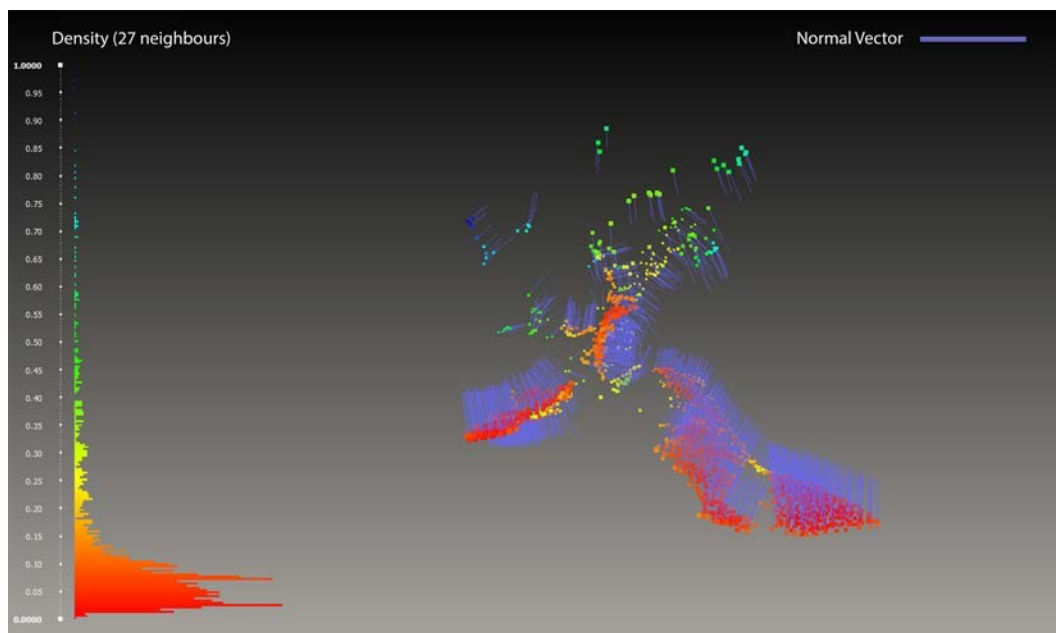


Figure 3: Some vegetation components remain in the Monfaucon scene after roughness segmentation, but can be distinguishes on density and normal orientation coherence.

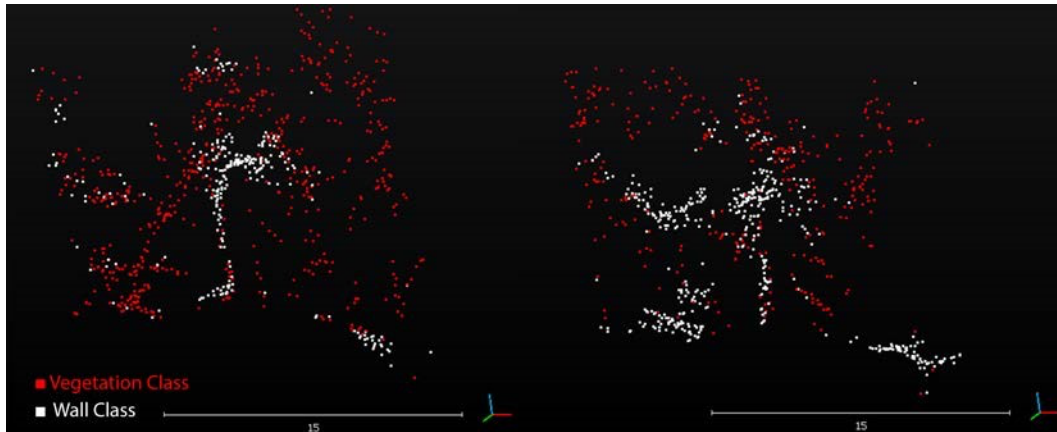


Figure 4: Profile slices after CANUPO classification.

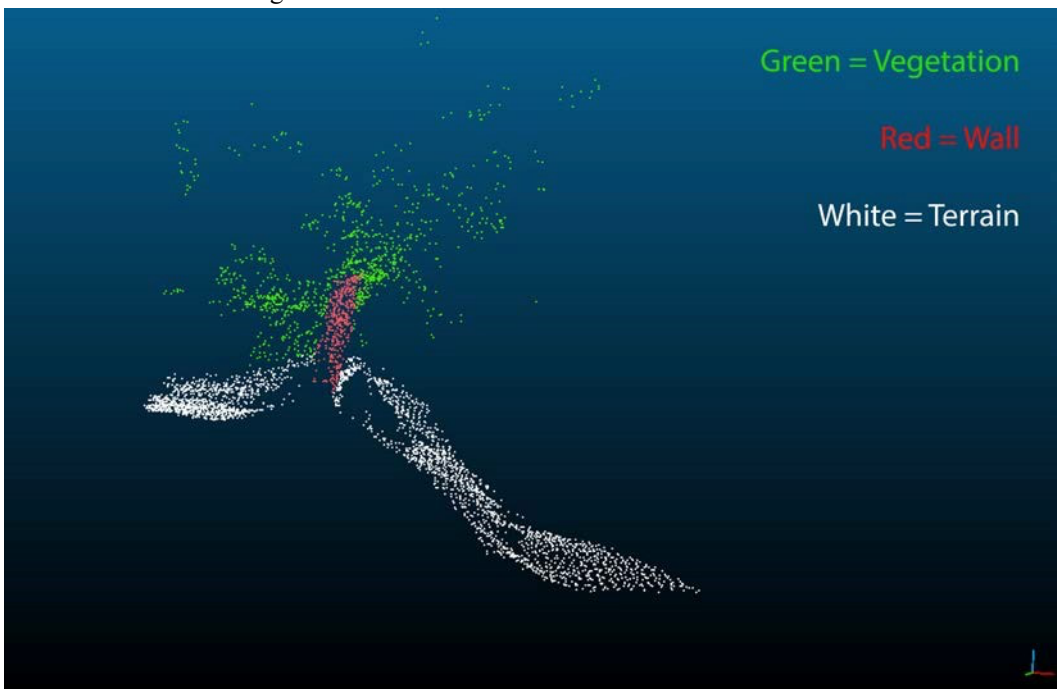


Figure 5: Final segmentation of the Montfaucon scene.

3.2 Bregille

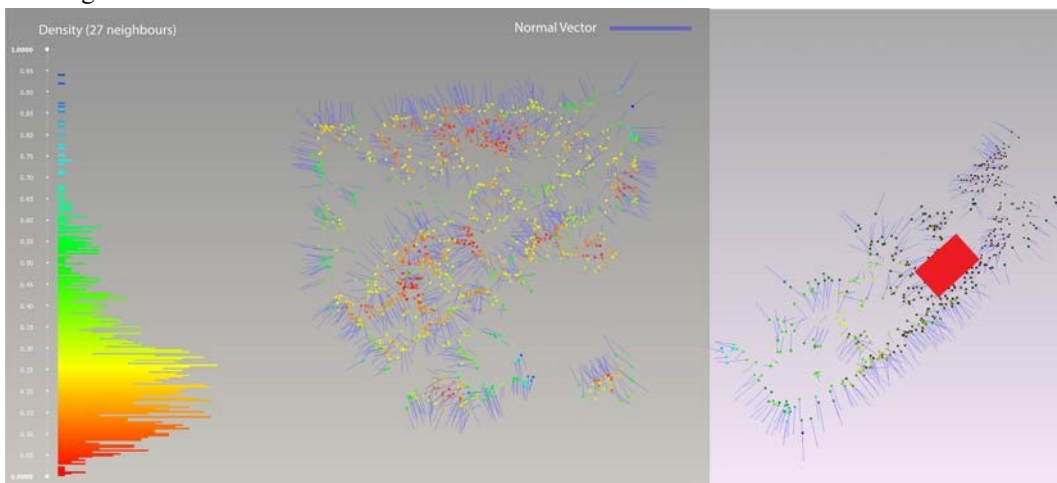


Figure 6. (a, left) Points coloured by density and normal direction represented as vectors. Individual walls are distinguished in this example on the basis of normal orientation. (b, right) The results of the CANUPO classification as an alternative first step. The rectangle marks the location of some mis-classified terrain points. Again, Individual walls are distinguished in this example on the basis of normal orientation

3.2.1 Results with the primary method

The remains at Bregille are, as for the Montfaucon scene, initially segmented based on roughness values, iterating over the point cloud at scales $S1=5m$, $S2=3m$, and $S3=11m$. Two vegetation components remain. The local density values for the remaining points are calculated, and points with density values falling outside 2σ of the density distribution are classified as vegetation and removed. At this point only returns from the terrain and the standing remains are present in the point cloud.

Terrain points, as identified in the initial TerraScan classification, are removed and the standing remains can be segmented into individual walls based on normal orientation (figure 6a). Some misclassified terrain points remain after the density segmentation and removal of TerraScanclassified terrain points, but these can be distinguished on the basis of their normal orientation, strongly along the z-axis.

3.2.2 Alternative calculations based on CANUPO

To demonstrate the robustness of our approach to variations in the calculation of dimensionality, we classified the Bregille scene using CANUPO. Spatial scales between 1m and 10m were used, at 0.5m intervals on training datasets for 'wall', 'vegetation' and 'terrain'. As with our original calculations using roughness, these scales are defined based on the resolution of the data, size of the objects in each class, and preliminary tests at various scales to determine which produced the best separation between classes (following the data driven approach used by Brodu and Lague). The reported balanced accuracies for the classifications were very good ($ba>0.98$). The classification resulting from this step is in many ways similar to that from the roughness step in our standard approach, but we note edge effects at the limits of the dataset (figure 6a). Removing these edge areas leaves a 'walls' class similar to that obtained using the standard approach.

3.3 Chapelle des Buis

In this scene small walls, of less than 50cm in width and preserved to less than 1m in height are present among dense scrub, under a mixed deciduous canopy. In this case initial calculation of the roughness values at scales of 1, 3, 5, and 7 m reveal a different situation than at Montfaucon or Bregille. Here the lowest roughness values correspond predominantly to the understory canopy rather than to the terrain (figure 7).

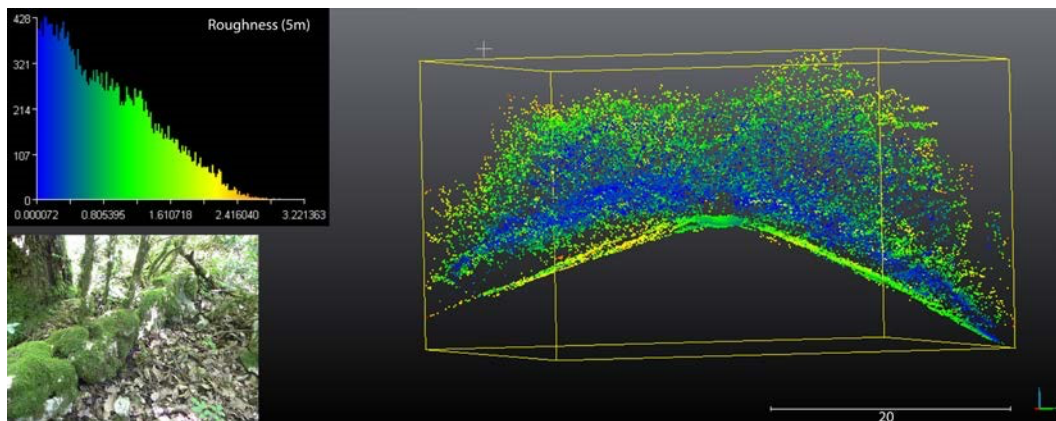


Figure 7. Dominant vegetation in this scene results in the lowest roughness values at the 5m scale (shown here) appearing in the understory canopy, and higher roughness values appearing on the terrain and standing archaeological remains.

It is clear from this initial step that the approach taken at Montfaucon and Bregille will not succeed in this case, due to the extremely dense understory combined with the small scale of the features present. Rather than removing points with roughness values beyond 1σ in the roughness distribution, we invert the procedure and retain these points. The result is a point containing the majority of the terrain points and a number of vegetation components.

The usual procedure is now followed, segmenting the cloud on roughness, local point density, and normal orientation. The resulting point cloud does not contain concentrations of low roughness returns with coherently oriented normals. Visits to the site reveal structures (figure 7, inset) were not identified using the proposed approach. Based on a visual inspection of the point cloud we conclude that the small number of returns from these structures, fewer than 12 on a typical wall, combined with a strongly structured vegetation canopy, prevents their successful identification using this approach.

4. RESULTS

In this paper three scenes were used to demonstrate an approach to the identification of standing architectural remains in mixed natural scenes using purely geometric measures of the point cloud. Using data collected at 8 pts/m² standing architectural remains at the 2-3m scale (vertical height) are successfully identified in medium density understory beneath a deciduous canopy. However, smaller remains, of less than 1m in height and located in dense understory canopy, are not detected regardless of the metric used for spatial dimensionality. We predict that remains on this scale would be detected under similar vegetation conditions with ALS data collected at a higher point density.

5. DISCUSSION

The principles of distinguishing standing archaeological remains, terrain and vegetation in ALS data by using local measures of dimensionality (roughness or PCA), density and normal orientation are illustrated in this paper. The results presented here show that a combination of metrics results in a better classification than the use of a single multi-scale metric. For example, after the classification of the Bregille scene based on multi-scale roughness or dimensionality as calculated in CANUPO, some vegetation points are present in the segmented point cloud, which should only contain terrain and standing remains' points. However, further segmentation on the basis of point density allows us to correctly identify these points as vegetation.

Sloping or otherwise varied terrain and standing architectural components of the point cloud can have very similar roughness values across multiple scales, but can be clearly distinguished based on dominant normal direction because terrain components will have normals predominantly oriented towards the z-axis (except on extremely steep slopes) and standing architectural components will have normals predominantly oriented in the plane of the x-y axes. Even in the cases of relatively steep local slopes, as seen at Montfaucon (figure 3) the normals on the sloping terrain are oriented more strongly toward the z-axis than the normals from architectural components. This allows for successful segmentation into connected components and discrimination based on dominant normal orientation. In conclusion, we emphasize the flexibility and robustness of the proposed approach, as demonstrated by the parallel tests in the Bregille and Montfaucon case studies in which we use both CANUPO and the traditional roughness metric. The approach is, as explained above, robust to the details of the metric used, which is beneficial as researchers may implement it in software with variations on algorithms and are not restricted to using the programs used here. The principles of combining metrics for dimensionality (roughness), density and normal orientation, and the opening operation within the multi-scale dimensionality calculation, are the core of the proposed method.

ACKNOWLEDGEMENTS

This research was carried out within the LIEPPEC Project, supported by the Region de FrancheComte and the Observatoire des Dynamiques Industrielles et Territoriales (ODIT): Construction Historique des Espaces Forestiers (CHEF) program, generously supported by the EU Feder program. The authors gratefully acknowledge the support of both organizations.

REFERENCES

- [1] Opitz, R. and Cowley, D. (eds.), *Interpreting Archaeological Topography – 3D Data, Visualization and Observation*, Oxbow Books, Oxford, 2013.
- [2] Lekson, S. (ed), *The Architecture of Chaco Canyon, New Mexico*. University of Utah Press, 2007.
- [3] Chase, A. et al., Airborne LiDAR, archaeology, and the ancient Maya landscape at Caracol, Belize. *Journal of Archaeological Science*, 38(2), February 2011, Pages 387–398.
- [4] Dumarçay, J., and Royère, P., *Cambodian architecture: Eighth to thirteenth centuries*, Brill, 2001.
- [5] Doneus, M., Briese, C., Fera, M., and Janner, M., Archaeological Prospection of Forested Areas Using Fullwaveform Airborne Laser Scanning. *Journal of Archaeological Science*, 35 (4), 2008, 882–893.
- [6] Lasaponara, R., and Masini, N., Full-waveform Airborne Laser Scanning for the Detection of Medieval Archaeological Microtopographic Relief, *Journal of Cultural Heritage* 10 (Supplement 1), 2009, 78–82.
- [7] Opitz, R., *Lidar Applications in Archaeology*. Doctoral Thesis. University of Cambridge, Cambridge, 2009, 289–341.
- [8] Axelsson, P., DEM generation from laser scanner data using adaptive TIN models. *International Archives of Photogrammetry and Remote Sensing*, 33 (B4-1), 2000, 110-117.
- [9] Opitz, Rachel, and Laure Nuninger. "Point Cloud Metrics for Separating Standing Archaeological Remains and Low Vegetation in ALS Data." *Int. Arch. Photogramm. Remote Sens. Spatial Inf. Sci.*, 40, 2013, 459-464.
- [10] Sithole, G., & Vosselman, G., Experimental comparison of filter algorithms for bare-Earth extraction from airborne laser scanning point clouds. *ISPRS Journal of Photogrammetry and Remote Sensing*, 59(1), 2004, 85101.

- [11] Meng, X., Currit, N., & Zhao, K., Ground filtering algorithms for airborne LiDAR data: a review of critical issues. *Remote Sensing*, 2(3), 2010, 833-860.
- [12] Sithole, G., & Mapurisa, W., 3D Object Segmentation of point clouds using profiling techniques. *South African Journal of Geomatics*, 1(1), 2012, 60-76.
- [13] Mallet, C., & Bretar, F., Full-waveform topographic lidar: State-of-the-art, *ISPRS Journal of Photogrammetry and Remote Sensing*, 64(1), 2009 1-16.
- [14] Niemeyer, J., Rottensteiner, F., & Soergel, U., Contextual classification of lidar data and building object detection in urban areas. *ISPRS Journal of Photogrammetry and Remote Sensing*, 87, 2014, 152-165.
- [15] Rottensteiner, F., Advanced methods for automated object extraction from LiDAR in urban areas. In *Geoscience and Remote Sensing Symposium (IGARSS)*, 2012, 5402-5405.
- [16] Lague, D. and Brodu, N., 3D terrestrial lidar data classification of complex natural scenes using a multi-scale dimensionality criterion: Applications in geomorphology, *ISPRS Journal of Photogrammetry and Remote Sensing*, 68, 2012., 121-134.
- [17] Lague, D., Brodu, N. and Leroux, J., Accurate 3D comparison of complex topography with terrestrial laser scanner: Application to the Rangitikei canyon (N-Z), *ISPRS Journal of Photogrammetry and Remote Sensing*, 82, 2013, 10-26.
- [18] Keller, W. and Borkowski, A., Wavelet based buildings segmentation in airborne laser scanning data set, *Geodesy and Cartography*, 60 (2), 2012, 99-121.
- [19] Niemeyer, J., Rottensteiner, F., & Soergel, U., Contextual classification of lidar data and building object detection in urban areas. *ISPRS Journal of Photogrammetry and Remote Sensing*, 87, 2014, 152-165.
- [20] Neidhart H., Sester M., Extraction of buildings ground planes from LiDAR data, *International Archives of the Photogrammetry, Remote Sensing and Spatial Information Sciences*, Vol. XXXVII, Part B2, 2008., 405–410.
- [21] Mei Quang, W., Skands, U., & Conradsen, K., Evaluation of fracture roughness using two kinds of fractal dimension measurements. *Acta Stereologica*, 14(1), 2014, 45-50.
- [22] Brubaker, K. M., Myers, W. L., Drohan, P. J., Miller, D. A., & Boyer, E. W. , The Use of LiDAR Terrain Data in Characterizing Surface Roughness and Microtopography. *Applied and Environmental Soil Science*, 2013, doi:10.1155/2013/891534.
- [23] Croft, H., Anderson, K., Brazier, R. E., & Kuhn, N. J., Modeling fine scale soil surface structure using geostatistics. *Water Resources Research* 2013.
- [24] Glenn, N. F., Streutker, D. R., Chadwick, D. J., Thackray, G. D., & Dorsch, S. J., Analysis of LiDAR-derived topographic information for characterizing and differentiating landslide morphology and activity. *Geomorphology*, 73(1), 2006, 131-148.
- [25] Brubaker, K., Myers, W., Drohan, P., Miller, D., and Boyer, E., The Use of LiDAR Terrain Data in Characterizing Surface Roughness and Microtopography, *Applied and Environmental Soil Science*, 2013.
- [26] Ma, J., Feng, H. Y., & Wang, L., Normal Vector Estimation for Point Clouds via Local Delaunay Triangle Mesh Matching. *Computer-Aided Design and Applications*, 10(3), 2013, 399-411.
- [27] Klasing, K., Althoff, D., Wollherr, D., & Buss, M., Comparison of surface normal estimation methods for range sensing applications. In *Robotics and Automation, ICRA'09. IEEE International Conference*, 2009, 3206-3211.
- [28] Milazzo, Lorenzo. "Multifractal analysis of three-dimensional grayscale images: Estimation of generalized fractal dimension and singularity spectrum." *arXiv preprint arXiv:1310.2719*, 2013.
- [29] Sim, K., Aung, Z. and Gopalkrishnan, V., Discovering Correlated Subspace Clusters in 3D Continuous-Valued Data, *Proceedings of the ICDM*, 2010, 471-480.
- [30] Vetter, M., et al., Vertical Vegetation Structure Analysis and Hydraulic Roughness determination using dense ALS point cloud data- a voxel based approach. *International Archives of Photogrammetry, Remote Sensing and Spatial Information Sciences*, XXXVIII (Part 5/W12), 2011, 1-6.
- [31] Ferraz, A., Bretar, F., Jacquemoud, S. Concalves, G. and Pereira, L., 3D segmentation of forest structure using an adaptive mean shift based procedure, in *Proceedings of SilviLaser 2010: The 10th International Conference on LiDAR Applications for Assessing Forest Ecosystems*, 2010, 280-290.
- [32] Richter, R., Behrens, M., & Döllner, J., Object class segmentation of massive 3D point clouds of urban areas using point cloud topology. *International Journal of Remote Sensing*, 2013, 34(23), 8408-8424.
- [33] CloudCompare (version 2.4) [GPL software]. EDF R&D, Telecom ParisTech (2013). Retrieved from <http://www.danielgm.net/cc/>.
- [34] MeshLab (version 1.32) [GPL software]. Visual Computing Lab - ISTI – CNR (2013) Retrieved from <http://meshlab.sourceforge.net/>.